Journal of Biomedical Optics

BiomedicalOptics.SPIEDigitalLibrary.org

Viscous optical clearing agent for *in vivo* optical imaging

Zijian Deng
Lijia Jing
Ning Wu
Pengyu lv
Xiaoyun Jiang
Qiushi Ren
Changhui Li

SPIE.

Viscous optical clearing agent for *in vivo* optical imaging

Zijian Deng,[a] Lijia Jing,[b] Ning Wu,[a] Pengyu Iv,[c] Xiaoyun Jiang,[a] Qiushi Ren,[a] and Changhui Li[a,*]
[a]Peking University, College of Engineering, Department of Biomedical Engineering, No. 5 Yiheyuan Road, Haidian, Beijing 100871, China
[b]Harbin Institute of Technology, School of Life Science and Technology, Harbin 150001, China
[c]Peking University, College of Engineering, Department of Mechanics and Engineering Science, Beijing 100871, China

Abstract. By allowing more photons to reach deeper tissue, the optical clearing agent (OCA) has gained increasing attention in various optical imaging modalities. However, commonly used OCAs have high fluidity, limiting their applications in *in vivo* studies with oblique, uneven, or moving surfaces. In this work, we reported an OCA with high viscosity. We measured the properties of this viscous OCA, and tested its successful performances in the imaging of a living animal's skin with two optical imaging modalities: photoacoustic microscopy and optical coherence tomography. Our results demonstrated that the viscous OCA has a great potential in the study of different turbid tissues using various optical imaging modalities. © *2014 Society of Photo-Optical Instrumentation Engineers (SPIE)* [DOI: 10.1117/1.JBO.19.7.076019]

Keywords: optical clearing; photoacoustic microscopy; optical coherent tomography; optical imaging; ultrasonic coupling.

Paper 140400R received Jun. 23, 2014; revised manuscript received Jul. 4, 2014; accepted for publication Jul. 9, 2014; published online Jul. 28, 2014.

1 Introduction

By smoothing the refractive index, optical clearing agents (OCAs) can effectively reduce tissue light scattering.[1,2] Since OCAs can make the skin more "transparent," they are commonly employed in many optical imaging modalities, such as optical coherence tomography (OCT),[3,4] two-photon microscopy,[5] and second harmonic generation imaging.[6] Recently, OCA was also implemented in another emerging optical imaging method, photoacoustic microscopy (PAM),[7,8] and *in vivo* photoacoustic flow cytometry.[9] In addition to developments in applications, more chemical components and new preparation methods make OCAs less toxic and more suitable for *in vivo* study.

However, commonly used OCAs primarily have high fluidity, which can easily flow away from the oblique, uneven, or moving surfaces of living bodies. Therefore, repeatedly reapplying agents during the experiments is generally required. Practically, this operation not only probably alters the morphology of the imaged target but also has the risk to change the alignment of the imaging system. Therefore, a viscous OCA for long lasting application on oblique, uneven, or moving surfaces, like the water-based ultrasonic coupling gel used in ultrasound imaging, is highly desired.

In this work, we developed an OCA with high viscosity. This agent can stay on a skin surface for a much longer time with little sacrifice of the optical clearing effect. In the following, we first described the preparation of this agent, and then measured its physical properties, followed by *in vivo* animal experiments with two optical imaging modalities to demonstrate its performance. Finally, we discussed the toxicity and other alternative methods to make viscous OCAs.

2 Methods and Results

2.1 *Preparation of the Viscous OCA*

The viscous OCA is composed of an OCA,[10] polyethylene glycol (PEG)400 (Sinopharm Chemical Reagent Co., Ltd., Beijing, China) mixed with thiazone (Yuancheng Gongchuang Technology Co., Ltd., Wuhan, China), a penetration enhancer, with the volume ratio of 9∶1. To increase the viscosity, 5% (mass percent) polyvinylpyrrolidone (PVP) K88-92 (Aladdin Industrial Co., Ltd., Shanghai, China) was added to the mixture as a thickener.

Due to the low dissolution rate of PVP K88-92 in PEG-400, we used water bath heating for PVP dissolution. To avoid possible chemical reactions related to thiazone at high temperature, thiazone was not put into the mixture while heating. After pouring PEG-400 into a beaker containing PVP and a magnetic stirrer, we rotated the magnetic stirrer immediately to disperse PVP. The mixture was kept at 95°C with stirring until all PVP was dissolved. Then, we cooled it slowly down to room temperature (~25°C). Thiazone was then added into the mixture with stirring. Due to the high viscosity of the mixture at room temperature, glass rod stirring by hand was performed until all the thiazone was dissolved.

2.2 *Characteristics of the Viscous OCA*

We used a rheometer (AR-G2, TA Instruments, Elstree, Herts, United Kingdom) to measure the viscosity of this viscous OCA, and compared it with that of PEG-400+thiazone (PEG-T, volume ratio of 9∶1). Newton's law of internal friction, which is obeyed by all Newtonian fluids, indicates that the viscosity of a lowly viscous fluid is the ratio of the shear stress to the shear rate, which is independent on the shear rate. Different from invariable viscosity (~0.09567 Pa · s) of PEG-T, which

*Address all correspondence to: Changhui Li, E-mail: chli@pku.edu.cn

0091-3286/2014/$25.00 © 2014 SPIE

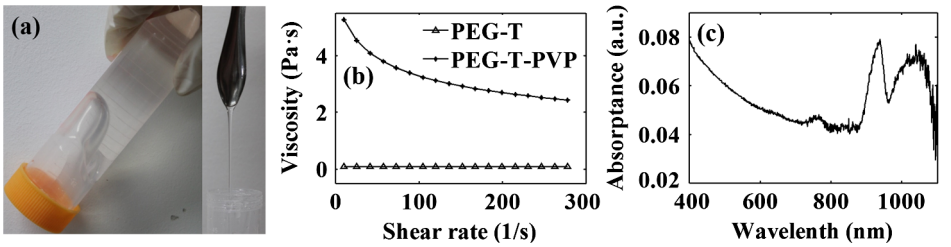

Fig. 1 (a) The photographs of PEG-T-PVP in viscous state. (b) The viscosities of PEG-T and PEG-T-PVP at different shear rate. (c) The absorption spectrum of PEG-T-PVP at 400 to 1100 nm.

was proven to be a Newtonian fluid, the viscosity of PEG-400 +thiazone+PVP (PEG-T-PVP) depended highly on the changes of the shear rate [shown in Fig. 1(b)], which means that the substance is too viscous to obey Newton's law of internal friction. Considering the low shear rate of the viscous OCA in practical experiment conditions, the viscosities at 10.00 1/s shear rate were chose for comparison. The viscosity of the new agent was 5.268, which is about 55-fold times that of PEG-T (0.09599). The viscosity of the mixture can be adjusted by changing the percentage of PVP in the mixture.

Optical properties of this OCA were measured. The optical refractive index of PEG-T-PVP was measured to be 1.477, which was similar to PEG-T (1.474), and was a bit larger than that of PEG-400 (1.465). The UV-vis absorption spectrum of the new agent was measured on a UV-vis spectrophotometer (Evolution 220, Thermo Scientific, Shanghai, China) in Fig. 1(c), which shows a small optical absorption from 400 to 1100 nm.

We also measured the relative acoustic attenuation of PEG-T-PVP at 20 MHz. In this measurement, PEG-T-PVP, water-based ultrasonic coupling gel, and deionized (DI) water, were successively filled into a container with 14-mm inner bottom diameter, 13-mm inner height. An unfocused ultrasound transducer (central frequency: 20 MHz; V-212-BB-RM, Olympus, Waltham, Massachusetts) contacted the top surface of the agents and detected the pulse-echo ultrasound signals passing through the agents. The amplitude ratio of the signal from the PEG-T-PVP to that from the DI water is 0.9132, which was similar to the ratio for gel (0.9609), so the PEG-T-PVP has a very low ultrasound attenuation as does the gel.

PEG-T has been proven to have a good optical clearing effect.[10] We tested the potential influence of additional PVP to the skin optical clearing effect. In this study, PEG-T-PVP and PEG-T were applied to two different pieces of *ex vivo* ventral skin from the same rat with thicknesses of about 1.13 and 1.09 mm, respectively. Figure 2(a) shows the setup of this experiment. A He-Ne laser at 632.8 nm was used as the light source. The light was expanded through a concave lens, then

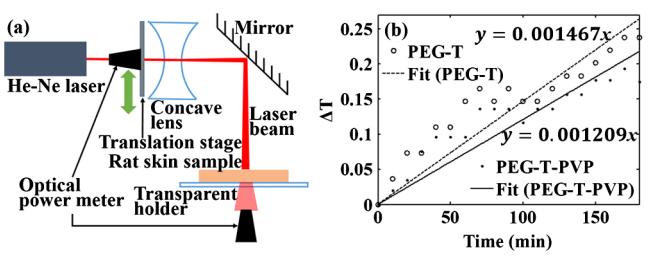

Fig. 2 (a) The experiment setup of PEG-T-PVP and PEG-T applied to *ex vivo* rat skin. (b) The ΔT of *ex vivo* rat skin with two different agents and corresponding fitted curves $y = Ax$.

shone on the rat skin. Two optical power meters (sensors: OP-2 VIS; LabMax_TOP, Coherent, Santa Clara, California) were used to detect the intensity of the transmitted light through the skin and also to monitor the variation of light intensity, respectively. The relative change of transmittance at i min ΔT_i was calculated as

$$\Delta T_i = \frac{T_i - T_0}{T_0}, \tag{1}$$

where $T_i = P_{ti}/P_{si}$, P_{ti} is the power of transmitted light at i min; and P_{si} is the laser source power at i min. Figure 2(b) shows the skin optical clearing results of the two agents. The slope of the solid line (with PVP) is 0.8241-fold as much as that of the dashed line (without PVP), which means that the presence of PVP slightly decreases the skin optical clearing effect.

2.3 *In Vivo Animal Study*

We then employed this viscous OCA in the *in vivo* imaging of animal skin by PAM and OCT. Due to the high viscosity, no agent reapplying operation was employed in all the following experiments, which guaranteed system alignment and imaging consistency during the experiment. Furthermore, we tested massage which is a commonly used method to improve skin permeability, to help the optical clearing of this viscous OCA. All research complied with protocols approved by the Institutional Animal Care and Use Committee of Peking University.

2.3.1 *PAM study*

In this study, two PAM modalities, acoustic-resolution PAM (AR-PAM)[11] and optical-resolution PAM (OR-PAM),[12] were used to study the effect of OCA on both rat and mouse skins, which are common models for skin optical clearing study. The laser wavelengths in following experiments are 532 nm.

Details of the AR-PAM system and its operation can be found in previous literature.[13] The imaged rat (~120 g, SD) was first anesthetized, and then the imaging region was cleanly depilated and gently scrubbed with DI water to remove impurities on the skin. Anesthesia was maintained by an isoflurane machine (1.0% to 1.2% vaporized isoflurane with an airflow rate of 1 L/min) throughout the experiment. An excessive amount of OCA was applied on its ventral skin before imaging. After a 5-min system alignment, we repeatedly scanned along a fixed line for 20 times to acquire a series of B-scan images. The interval between two successive scannings was 30 min. The wave-like patterns in Figs. 3(a) and 3(b) were induced by the rat's breathing motion during scanning. In this study,

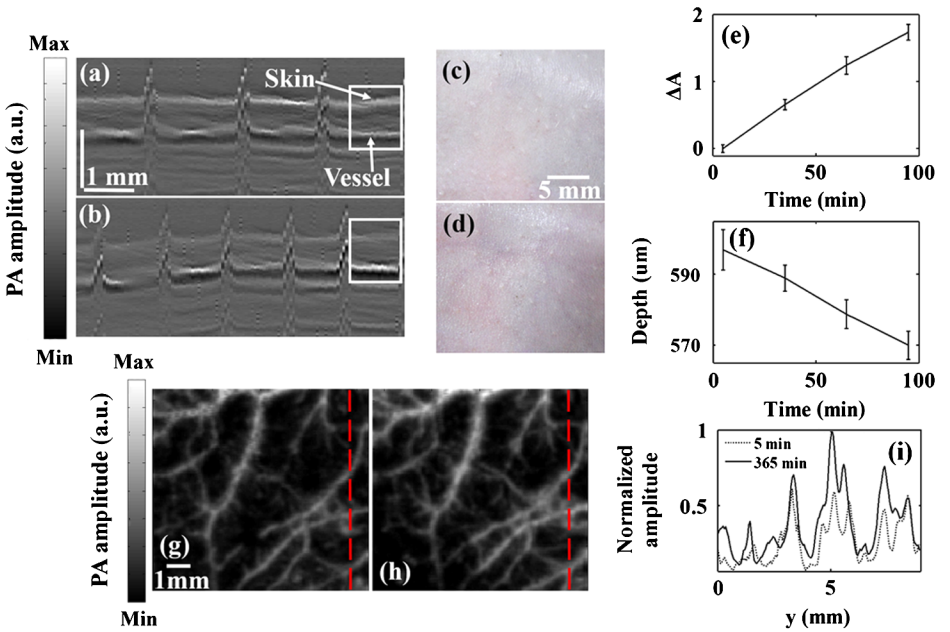

Fig. 3 AR-PAM B-scan images of rat skin after (a) 5 min and (b) 95-min PEG-T-PVP application, respectively. Panels (c) before and (d) after 95-min PEG-T-PVP application, respectively. (e) The ΔA of selected vessel from B-scan images. (f) The depth between the surface of the skin and the selected vessel from B-scan images. Maximal amplitude projection (MAP) images of another rat skin after (g) 5 min and (h) 365-min PEG-T-PVP application, respectively. (i) Normalized PA amplitude along the red dashed line in (g) and (h).

a 20-frame-mean amplitude (A_i) from a selected subcutaneous blood vessel [shown in Figs. 3(a) and 3(b)] at i min was calculated. ΔA_i, the relative change of A_i, was processed similar to Eq. (1). Figure 3(e) demonstrated the obvious increase in PA amplitudes from the selected vessel. In addition, we measured the depth from the skin top surface to the center of the selected vessel in the selected region. Figure 3(f) shows the decrease of the depth. It is consistent with the skin thinning effect due to dehydration caused by the hypertonicity of PEG-400. Maximal amplitude projection (MAP) images of another rat skin with an application of viscous OCA were also obtained. As shown in Figs. 3(g) and 3(h), not only do the PA amplitudes of shallow subcutaneous vessels become stronger, but more branching vessels in deeper regions were also visualized. The ΔA of five randomly selected subcutaneous blood vessels from MAP images (from 5 to 365 min, 60-min interval) monotonically increased as in Fig. 3(e).

We also compared the performance between the viscous OCA and water-based ultrasonic coupling gel in an *in vivo* mouse (~25 g, BALB/c) skin study. The content of vaporized isoflurane for mice was decreased from 0.8% to 1.0%. Contrary to the increases when using the viscous OCA, the PA amplitude from subcutaneous vessels decreased using the traditional water-based gel [shown in Fig. 4(e)], which demonstrated that the skin whitening induced by gel could impact the penetration of light. In addition, using water-based gel made the distances between epidermis and the subcutaneous blood vessel larger, as shown in Fig. 4(f). The gel was hypotonic versus skin, which fosters the diffusing of water from the gel into the skin, allowing the skin to become whiter and thicker.

In the OR-PAM, the lateral resolution is determined by t diffraction-limited optical focusing, while the focusing capability degrades due to tissue optical scattering. We tested the performance of this viscous OCA in an OR-PAM study of a living mouse (~25 g, BALB/c). Details of the OR-PAM system and its operation can be found in other literature.[14] The increase of amplitudes from subcutaneous blood vessels was seen in Fig. 5(c). The MAP images were acquired after 5 and 65 min applications of the new OCA, as shown in Figs. 5(d) and 5(e). The FWHMs of the Gaussian fit was calculated along the red dashed lines on the two vessels [seen in Figs. 5(f) and 5(g)].

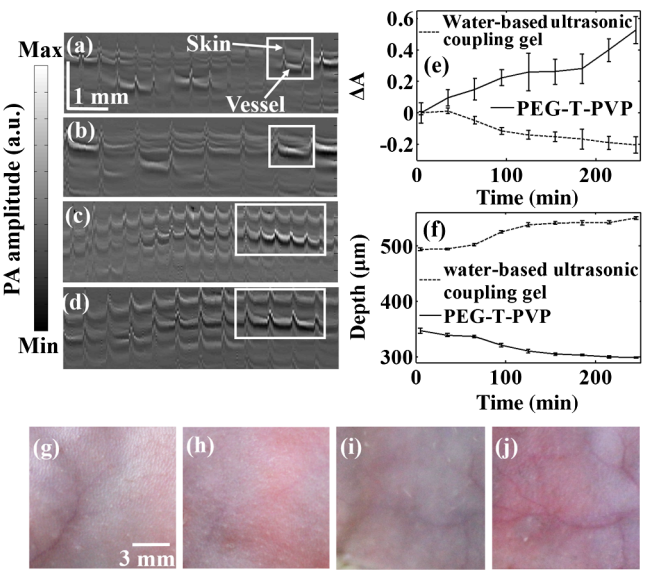

Fig. 4 AR-PAM B-scan images of mice skin after (a) and (c) 5 min, (b) and (d) 245-min PEG-T-PVP application and water-based ultrasonic coupling gel application, respectively. (e) The ΔA of selected vessels from B-scan images. (f) The depth between the surface of the skin and the selected vessel from B-scan images. Panels (g) and (i) before, (h) and (j) after 245-min PEG-T-PVP and gel application, respectively.

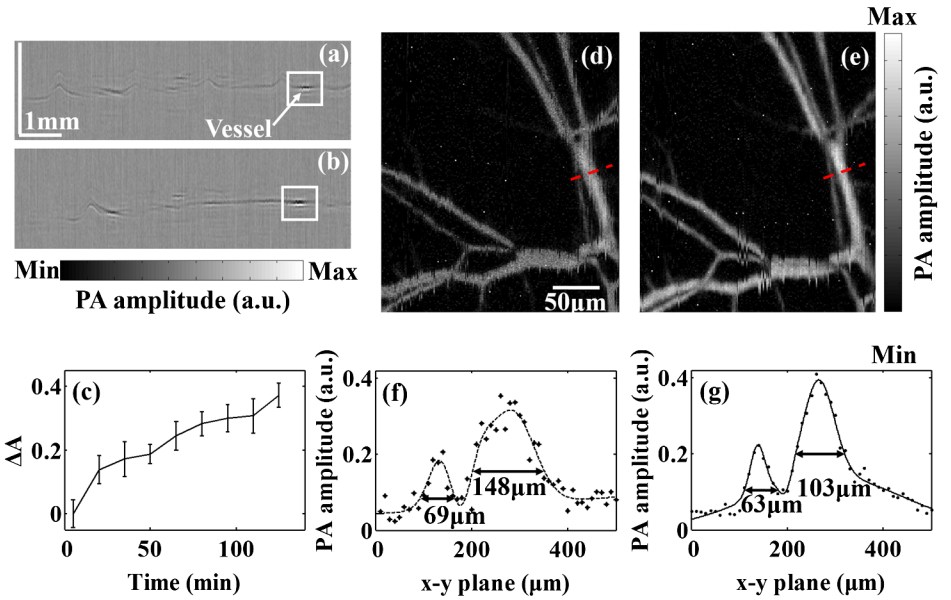

Fig. 5 OR-PAM B-scan images of mouse skin after (a) 5 min, and (b) 125-min PEG-T-PVP application, respectively. (c) The ΔA of selected vessel from B-scan images. MAP images of another mouse skin after (d) 5 min and (e) 65-min PEG-T-PVP application, respectively. The FWHMs of Gaussian fit (f) and (g) along red dash lines in (d) and (e), respectively.

Not only did the PA amplitudes of the two vessels increase, but the FWHMs of the two vessels noticeably decreased, which verified that viscous OCA can improve the lateral resolution of OR-PAM.

2.3.2 *OCT study*

OCA has already been successfully implemented in OCT.[15] To validate the performance of this viscous OCA, we used it in *in vivo* rat skin imaging with a commercial OCT system (central wavelength: 840 nm, OCT1000, New Vision, Dongguan, China). The preparation of rat (~120 g, SD) skin and animal anesthesia was similar to the aforementioned procedure. After application of the viscous OCA on rat skin, we scanned the rat skin every 15 min, and at each scanning 32 B-scan images were acquired. Five of each of the 32 B-scans were randomly selected on which to perform statistical analysis [as shown in Figs. 6(a) and 6(b)]. Details of the processing method for selected regions can be found in the previous literature.[15] The total attenuation coefficient μ_t was gained from the fitted curve of the averaged OCT signals shown in Figs. 6(c) and 6(d). $\Delta\mu_t$, the relative change of μ_t, was processed similarly to

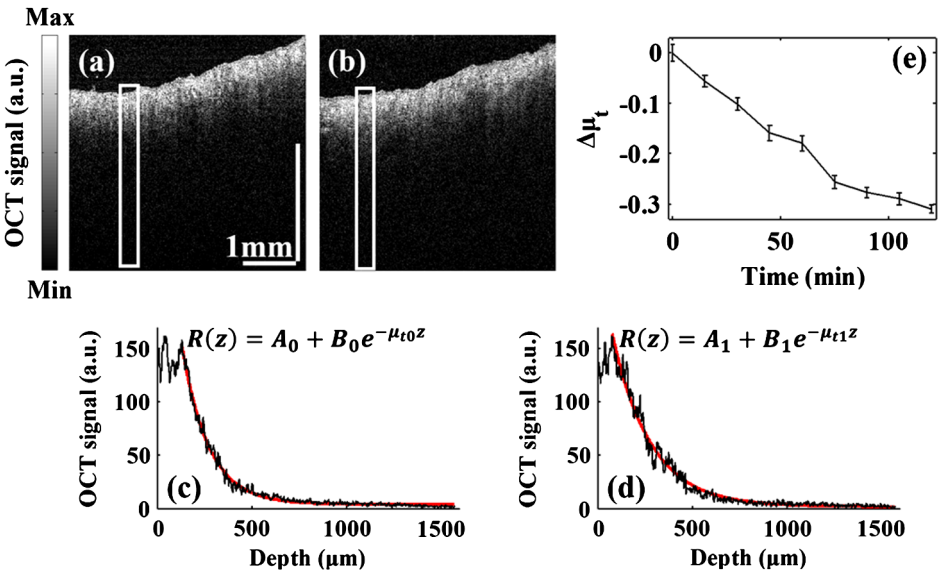

Fig. 6 OCT B-scan images of rat skin after (a) 0 min and (b) 120-min PEG-T-PVP application, respectively. Panels (c) and (d) the averaged OCT in-depth signal of respectively selected regions from (a) and (b) and corresponding fitted curves $R(z) = A + Be^{-\mu_t z}$, where $A_0 = 4.156$, $B_0 = 149.1$, $\mu_{t0} = 70.76\ \text{cm}^{-1}$, and $A_1 = 1.987$, $B_1 = 161.8$, $\mu_{t1} = 49.03\ \text{cm}^{-1}$. (e) The $\Delta\mu_t$ of selected region from five random B-scans.

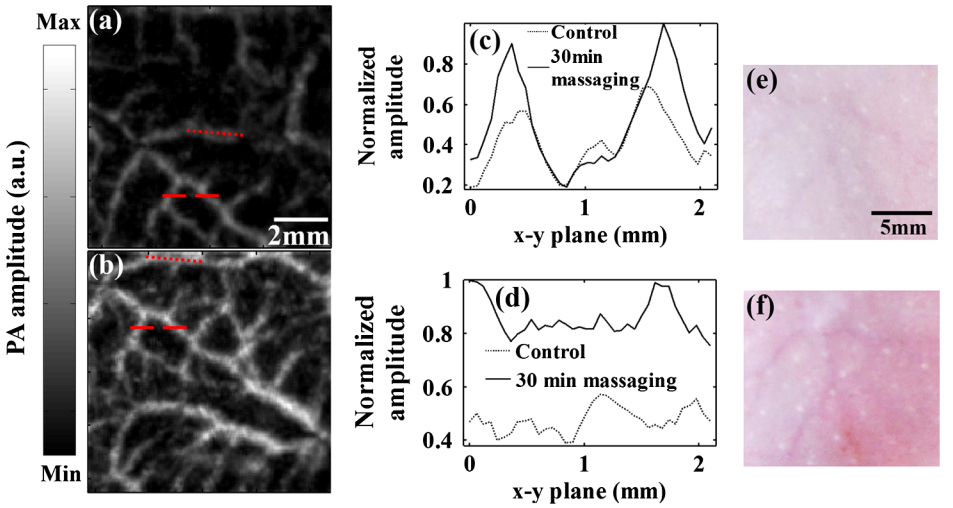

Fig. 7 MAP images of another rat skin (a) before and (b) after 30-min PEG-T-PVP application with massage, respectively. Normalized PA amplitude along the (c) red dashed line and (d) red dotted line in (g) and (h), respectively. Panels (e) before and (f) after 30-min PEG-T-PVP application with massage, respectively.

Eq. (1) using $\bar{\mu}_{ti}$, the μ_t mean of 5 frames at i min. Figure 6(e) demonstrated the decrease of μ_t of rat skin.

2.3.3 *Performance of massage for viscous OCA*

As is commonly employed in the implementation of OCAs,[8,9] massage was used as an effective way to foster the optical clearing effect. Therefore, we also tested the effect of massage in helping the penetration of the viscous OCA when using the AR-PAM imaging system. In this study, we first acquired a control image of the rat (~120 g, SD) skin [seen in Fig. 7(a)] without OCA and massage. Then, the animal was removed from the AR-PAM system, and we applied the viscous OCA on the same site and performed massage for 30 min. After that, we repositioned the rat in the PAM system and did another imaging [as seen in Fig. 7(b)]. Compared with Fig. 7(a), Fig. 7(b) showed a dramatic enhancement in the photoacoustic signal. In addition, the time for the OCA to take effect was greatly shortened compared with the results in Figs. 3(g) and 3(h). Since massage slightly altered the morphology of the skin and the repositioning of the animal caused variations in the imaging area, the imaging region in Fig. 7(b) does not exactly match that in Fig. 7(a).

3 Conclusions and Discussions

In summary, we developed a viscous OCA composed of PEG-400, thiazone, and PVP. We demonstrated that this OCA has the combined good properties of high viscosity and an optical clearing effect. The high viscosity allows the OCA to be more stable on oblique, uneven, or moving skin surfaces, avoiding multiple reapplications of OCAs during the experiment. In addition, the new OCA overcomes the skin whitening effect of water-based ultrasonic coupling gel. In addition, our results also demonstrated that the massage operation successfully helps the performance of this viscous OCA. The toxicity of PEG-T has been tested in a previous study,[10] concluding that no apparent inflammatory or toxic reactions were induced. In addition, it has been confirmed that the PVP is a safe component often used in daily cosmetics.[16] As a nontoxic excipient to thicken the mixture without a chemical reaction, PVP does not affect the safety of the mixture.

In addition to the recipe and preparation method of the viscous OCA in this work, other chemical components and procedures are potential for viscous OCAs. Several OCAs,[2] which are widely used for optical clearing, can be components of viscous OCAs. Different penetration enhancers or thickeners also have the potential for the preparation of viscous OCAs. However, the solubility of penetration enhancers or thickeners in OCAs is the main challenge to preparation. For example, agarose, another polymer for thickening, is poorly soluble in PEG-400 and propylene glycol; thiazone is poorly soluble in glycerol at room temperature. We can choose an appropriate proportion among these three substances to gain a mixture sited to a specific application.

To the best of our knowledge, this is the first time an OCA with a high viscosity has been prepared. Our results showed that the imaging qualities in PAM and OCT can be improved using this viscous OCA. Other operations[17] for improving the skin permeability to OCA can be used for penetration enhancement before imaging. This viscous OCA has a great potential in the study of different turbid tissues using other optical imaging modalities, such as confocal or multiphoton microscopy and fluorescence imaging.

Acknowledgments

This work was sponsored by National Natural Science Foundation of China (Grant No. 61078073), the National Basic Research Program of China (973 Program, 2011CB707502), and the Guangdong Innovative Research Team Program (No. 2011S090).

References

1. V. V. Tuchin et al., "Light propagation in tissues with controlled optical properties," *J. Biomed. Opt.* **2**(4), 401–417 (1997).
2. D. Zhu et al., "Recent progress in tissue optical clearing," *Laser Photonics Rev.* **7**(5), 732–757 (2013).
3. S. G. Proskurin and I. V. Meglinski, "Optical coherence tomography imaging depth enhancement by superficial skin optical clearing," *Laser Phys. Lett.* **4**(11), 824–826 (2007).
4. X. Wen et al., "Enhanced optical clearing of skin in vivo and optical coherence tomography in-depth imaging," *J. Biomed. Opt.* **17**(6), 066022 (2012).

5. R. Cicchi et al., "Contrast and depth enhancement in two-photon microscopy of human skin ex vivo by use of optical clearing agents," *Opt. Express* **13**(7), 2337–2344 (2005).
6. S. Plotnikov et al., "Optical clearing for improved contrast in second harmonic generation imaging of skeletal muscle," *Biophys. J.* **90**(1), 328–339 (2006).
7. Y. Zhou, J. J. Yao, and L. H. V. Wang, "Optical clearing-aided photoacoustic microscopy with enhanced resolution and imaging depth," *Opt. Lett.* **38**(14), 2592–2595 (2013).
8. Y. Y. Liu et al., "Optical clearing agents improve photoacoustic imaging in the optical diffusive regime," *Opt. Lett.* **38**(20), 4236–4239 (2013).
9. Y. A. Menyaev et al., "Optical clearing in photoacoustic flow cytometry," *Biomed. Opt. Express* **4**(12), 3030–3041 (2013).
10. J. Wang, R. Shi, and D. Zhu, "Switchable skin window induced by optical clearing method for dermal blood flow imaging," *J. Biomed. Opt.* **18**(6), 061209 (2013).
11. K. Maslov, G. Stoica, and L. V. H. Wang, "In vivo dark-field reflection-mode photoacoustic microscopy," *Opt. Lett.* **30**(6), 625–627 (2005).
12. S. Hu, K. Maslov, and L. V. Wang, "Second-generation optical-resolution photoacoustic microscopy with improved sensitivity and speed," *Opt. Lett.* **36**(7), 1134–1136 (2011).
13. S. Ye et al., "Studying murine hindlimb ischemia by photoacoustic microscopy," *Chin. Opt. Lett.* **10**(12), 121701 (2012).
14. N. Wu et al., "High-resolution dual-modality photoacoustic ocular imaging," *Opt. Lett.* **39**(8), 2451–2454 (2014).
15. E. A. Genina et al., "Optical coherence tomography monitoring of enhanced skin optical clearing in rats in vivo," *J. Biomed. Opt.* **19**(2), 021109 (2013).
16. W. F. Bergfeld et al., "Final report on the safety assessment of polyvinylpyrrolidone (PVP)," *Int. J. Toxicol.* **17**(Suppl. 4), 95–130 (1998).
17. S. P. Chernova et al., "On the dynamics of optical clearing of human skin in vivo," *Proc. SPIE* **4162**, 227–235 (2000).

Zijian Deng is a graduate student at Peking University.

Lijia Jing is a graduate student at Harbin Institute of Technology.

Ning Wu is a graduate student at Peking University.

Pengyu Iv is a graduate student at Peking University.

Xiaoyun Jiang is a graduate student at Peking University.

Qiushi Ren is a professor and chair of the Department of Biomedical Engineering, Peking University.

Changhui Li is an associate professor of the Department of Biomedical Engineering, Peking University. He obtained his PhD in physics from Texas A&M University in 2006. His research interests include biomedical optics and molecular imaging.